Published paper
Korossis, S., Bolland, F., Southgate, J., Ingham, E. and Fisher, J. (2009)
Regional biomechanical and histological characterisation of the passive porcine urinary bladder: Implications for augmentation and tissue engineering strategies.
Biomaterials, 30 (2). pp. 266-275.

* Title Page

Regional Biomechanical and Histological Characterisation of the Passive Porcine Urinary Bladder: Implications for Augmentation and Tissue Engineering Strategies

Sotirios Korossis, PhD *(Corresponding Author)*

Institute of Medical and Biological Engineering

University of Leeds, Leeds, LS2 9JT, United Kingdom

E-mail: s.korossis@leeds.ac.uk

Tel. no: 0113 343 2197

Fax no: 0113 242 4611

Fiona Bolland, PhD

Jack Birch Unit of Molecular Carcinogenesis, Department of Biology, University of York, Heslington, York, YO10 5YW, United Kingdom.

Jenny Southgate, PhD

Jack Birch Unit of Molecular Carcinogenesis, Department of Biology, University of York, Heslington, York, YO10 5YW, United Kingdom.

Eileen Ingham, PhD

Institute of Medical and Biological Engineering, University of Leeds, Leeds, LS2 9JT, United Kingdom.

John Fisher, PhD, DEng

Institute of Medical and Biological Engineering, University of Leeds, Leeds, LS2 9JT, United Kingdom.

Abstract

The aim of this study was to identify and quantify potential regional and directional variations in the quasistatic uniaxial mechanical properties of the passive urinary bladder wall. Overall, the lower body and trigone regions demonstrated the highest degree of directional anisotropy, whereas the ventral region demonstrated the least directional anisotropy. Significant regional anisotropy was found only along the apex-to-base direction. The dorsal and ventral regions demonstrated a significantly increased distensibility along the apex-to-base direction compared to the other bladder regions, whereas the trigone and lower body regions demonstrated the least distensibility. The trigone, lower body and lateral regions also demonstrated the highest tensile strength both at regional and directional level. The study detected significant regional and directional anisotropy in the mechanical properties of the bladder and correlated this anisotropy to the distended and non-distended tissue histioarchitecture and whole organ mechanics. By elucidating the inhomogeneous nature of the bladder, the results from this study will aid the regional differentiation of bladder treatments in terms of partial bladder replacement with suitable natural or synthetic biomaterials, as well as the development of more realistic constitutive models of bladder wall biomechanics and improved computational simulations to predict deformations in the natural and augmented bladder.

Introduction

A variety of congenital and acquired conditions result in bladder dysfunction with consequent debilitating incontinence, which affects approximately 400 million people worldwide. In the majority of cases, a decrease in compliance is caused by thickening of the bladder wall due to smooth muscle cell hypertrophy and increased connective tissue deposition [1]. This may arise due to increased distension of the bladder wall (e.g. due to bladder outlet obstruction), which may directly or indirectly act as a stimulus for hypertrophy and hyperplasia [2,3,4,5]. Furthermore, neuropathic disease or trauma can induce significant alterations in the neural control of the bladder, which in turn can cause substantial changes in bladder function. These functional changes can produce severe alterations in the structure, thickness, compliance and biomechanics of the bladder wall [6,7,8]. Currently, the major surgical solution to restore lost function due to trauma, neurogenic or vascular dysfunction, or cancer is bladder augmentation surgery. Bowel is most commonly used in various procedures of neobladder replacement, such as augmentation enterocystoplasty or substitution enterocystoplasty. However, its use is not without long-term complications [9,10,11], suggesting that the materials used for the repair may be inadequate. In fact, rupture of the repaired bladder wall is known to occur in ~5% of cases [12].The lack of an entirely satisfactory clinical procedure has led researchers to pursue alternative bladder replacement materials involving tissue engineering techniques [13,14].

Ideal materials for complete or partial bladder replacement should possess both biological compatibility, to promote cellular and tissue integration, and mechanical reliability. In order to design more appropriate long-term surgical repair procedures and develop materials for bladder reconstruction, and indeed to gain an insight into

the disease processes that lead to bladder dysfunction, it is necessary to characterize and quantify the fundamental mechanical properties of the normal bladder at the mesoscale-tissue level and correlate them to both whole organ mechanics and tissue histioarchitecture. Quantitative linking of the mechanics to bladder histioarchitecture will also help to elucidate the repercussion of cellular and molecular level alterations on bladder function [15]. Along these lines, studies have correlated alterations in myosin isoform and collagen type content to force development in bladder muscle strips [16,17] or to urodynamics data [18,19]. Such correlations are important not only for interpreting structural/functional changes in studying patterns of bladder dysfunction, but also to predict the fate of replacement materials when exposed to the local normal or pathological mechanical loading in the bladder wall *in vivo*.

In addition to the active contraction of the detrusor smooth muscle, the bladder demonstrates nonlinear elastic, viscous and plastic mechanical properties [20,21,22,23,24,25,26], depending on the boundary conditions. However, during normal physiological filling rates bladder deformation can be considered quasistatic [27], whereas neural and contractile effects are minimal [28]. Over the years, several mathematical models have been developed in an effort to predict the stress-strain behaviour of the bladder wall. Most of these models assume isotropy, homogeneity, incompressibility and a spherical shape for the bladder wall [22,29,30,31]. Although the assumptions of a spherical shape and incompressibility can give a relatively good description of bladder mechanics during filling [32], it is questionable how descriptive are the assumptions of isotropy and homogeneity for the bladder wall. The bladder demonstrates a considerable inherent inhomogeneity in its material properties [33], and as a result, it does not stretch equally in all directions, demonstrating areas of

higher stretching and, subsequently, higher stress. In spite of this, relatively little is known about the anisotropic mechanical properties of the bladder wall in terms of direction or region, and only a meagre few studies have focused on this issue [34,35]. As a first step towards the development of tissue engineered bladder repair materials, the authors performed the first regional and directional mechanical characterisation of the urinary bladder. In particular, the objective of this study was to identify and quantify potential regional and directional variations in the passive mechanical properties of the bladder wall and correlate these variations to its histioarchitecture and whole organ mechanics. By elucidating the inhomogeneous nature of the bladder, the aim of this work was to consider the implications for developing suitable natural or synthetic biomaterials for bladder augmentation.

Materials & Methods

Specimen procurement & dissection

Intact bladders from 16-week-old commercial male pigs were collected from a local abattoir and transported to the laboratory on ice in transport medium [Hanks' balanced salt solution without Ca^{++} and Mg^{++} (HBSS, Invitrogen, Paisley, UK) containing 10 mM HEPES, pH 7.6 (Invitrogen) and 10 KIU/ml Aprotinin (Trasylol, Bayer, Berkshire, UK)] [36]. The absence of calcium in the solution helped ensure that the bladders were in an inactivated state and that no spontaneous contractions would occur during testing. Prior to testing, the bladders were sized by photographing them in their deflated/non-distended state (Figure 1). The recorded images of the bladders were calibrated and the maximum bladder width along the circumferential direction was measured using an image analysis software (Image Pro Plus™, MediaCybernetics®). The average size of the bladders used in this study was 68 ± 11.7 mm (mean ± 95% confidence interval, n = 6).

The bladders were subsequently dissected along the apex-to-base line, as show in Figure 2a, and samples were isolated from the dorsal, trigone, lateral, ventral and lower body regions of the wall, as well as along the apex-to-base (longitudinal) and transverse (circumferential) directions (Figure 2b). For the purpose of the biomechanical characterization, specimens measuring 20×5 mm were isolated using a purpose-built block cutter [37]. From each bladder, one apex-to-base and one transverse specimen were isolated from each one of the five anatomical regions. Samples from the five anatomical regions and along the two directions were also harvested for histological examination. Following isolation, the specimens were stored in transport medium and tested either biomechanically or histologically within 6 hours from slaughter.

Histological characterisation

Histological examination was performed on samples harvested along the apex-to-base and transverse directions from the five anatomical regions of the bladder wall, in order to analyse the general histioarchitecture, as well as the amount and orientation of elastin, collagen and smooth muscle. The samples were retrieved either from the procured empty bladders and fixed in 10% (v/v) neutral buffered formalin (NBF), or from a bladder that had been distended to the mean physiological capacity with 500 ml of 10% (v/v) NBF. Post-fixation, distended and non-distended samples were dehydrated and embedded in paraffin wax. Histological sections were stained with either Miller's stain to evaluate the content and distribution of elastin, Van Gieson's stain to evaluate the distribution of collagen and smooth muscle, or with haematoxylin and eosin (H&E) [38]. The stained sections were examined under light microscopy and photographed.

Biomechanical characterisation

Bladder wall strips were subjected to low-strain rate uniaxial tensile loading to failure in order to investigate potential regional variations in the passive stress strain-behaviour of the bladder wall. In addition, the directional anisotropy of the bladder wall was investigated by testing specimens along the apex-to-base and transverse directions. In total, 10 test groups of 6 specimens each were studied. Prior to testing, the thickness of the samples was measured at 6 points along their long axis using a gauge with a resolution of 0.01 mm (Mitutoyo, Andover, UK), and their average thickness (t) was recorded. Subsequently, the samples were mounted onto a purpose-built titanium holder. The holder was supported by a removable aluminium bracket that allowed alignment of the two holder grips, defined the gauge length of the specimens, and ensured that no load was imposed on the specimen until the start of the test [37]. The gauge length of the specimens was defined by a 10 mm wide central block separating the two holder parts and screwed onto the bracket. Once a sample was clamped onto the holder, the holder with the supporting bracket was secured to a Howden tensile machine and the bracket was removed. Prior to loading to failure, the specimens were preconditioned under cyclic loading using a double-ramp wave function at a rate of 10 mm/min. A preconditioning regime of 10 cycles was sufficient to produce a steady-state load-elongation response from the samples. Following preconditioning, the samples were sequentially stretched to failure at a rate of 10 mm/min. All testing was conducted in physiologic saline (0.9% w/v NaCl) and at room temperature. Total testing time was approximately 3 min per specimen. During testing, load data from the load cell and specimen extension data from the stroke of the cross-head of the tensile testing machine was acquired at a rate of 20Hz.

In order to obtain an accurate measure of the tissue gauge length, the tensile machine was set to produce a specimen preloading of 0.02 N before the operating program started to acquire any data. Therefore, zero extension was taken at the point where a load of 0.02 N was detected. The final gauge length (L_o) of the specimen was calculated as the initial gauge length (10 mm) plus the extension that was needed to produce the specified preloading. Failure was taken to occur when the first decrease in load was detected during extension. The mode of failure observed was middle section necking and rupture for all of the specimens tested. The recorded load (F) and specimen extension data (ΔL) from the loading to failure phase of each specimen was converted to stress and strain. Stress (σ) was defined in the Lagrangian sense as *F/unloaded cross-sectional area*, whereas the percentage in-plane axial strain (ε) was defined as $(\Delta L/L_o)\times 100\%$ [39]. The calculated stress-strain responses obtained for the specimens of each group were averaged over the number of specimens in each group (n = 6) using a mathematical analysis software package (Origin v6.0, Microbal). Moreover, the stress-strain behaviour of each specimen was analyzed by means of six parameters. These have been described elsewhere [37] and included the elastin (El-E) and collagen (Col-E) phase slopes, transition stress (σ_{trans}) and strain (ε_{trans}), ultimate tensile strength (σ_{uts}) and failure strain (ε_{uts}). The biomechanical parameters were analyzed by one-way analysis of variance (ANOVA) and the individual means from each group were compared using the Student's t-test to calculate the minimum significant difference at the 95% and 99% confidence levels.

In an attempt to link the passive mesoscale-tissue mechanical properties of the bladder wall obtained from the uniaxial tensile tests with the mechanics of the whole bladder, the calculated stress-strain data was converted to bladder intraluminal

pressure-bladder volume relationships using the law of Laplace for a thin-walled sphere. While no complete survey of bladder shapes was performed, the reports of the shapes of normal bladders tend to describe spherical bladders [40] and prolate spheroidal bladders [33]. Although these models are only rough approximations of the real bladder shape, it was deemed sufficient to use the spherical bladder assumption, together with the assumptions of homogeneity and isotropy entailed by the law of Laplace, to generate a qualitative correlation between mesoscale-tissue and organ scale properties. The purpose of this analysis was to examine how the whole bladder mechanics change if the regional and directional anisotropy inherent in the bladder wall is not taken into consideration.

The law of Laplace for a segment of homogeneous thin-walled sphere relates the internal pressure (P) applied to the segment, to its thickness (t) and radius (R), and the membrane stress (σ) in the segment, according to [41]:

$$P = \frac{2t\sigma}{R} \quad (1)$$

Assuming an un-pressurised bladder ark segment of angle θ and radius R_o, its original undeformed length is $L_o = R_o \cdot \theta$. When the segment is pressurised by an internal pressure P, its radius increases to R. In addition, its length increases by ΔL, generating an axial membrane stress (σ) along its length. The length of the pressurised segment is $L = L_o + \Delta L = R \cdot \theta$. Consequently, the radius R of the pressurised segment can be estimated by:

$$\frac{R}{R_o} = \frac{L_o + \Delta L}{L_o} = 1 + \varepsilon \quad (2)$$

L_o represents the un-stretched gauge length of the tissue specimens (final gauge length, allowing for the preloading of 0.02 N) used in the uniaxial tensile tests,

whereas the ratio $\Delta L/L_o$ is the in-plane axial strain (ε) in the segment and represents the strain calculated from the uniaxial tensile tests for the tissue strips. Therefore, the internal bladder pressure was calculated according to:

$$P = \frac{2t\sigma}{R_o(1+\varepsilon)} \quad (3)$$

The membrane stress σ, produced by the stretch ΔL in the bladder segment, represents the corresponding axial tensile stress calculated for the tissue strips under uniaxial tension. Moreover, the volume of the bladder, corresponding to the in-plane axial strain in the bladder segment, was estimated from the volume of the sphere and employing equation (2):

$$V = \frac{4}{3}\pi R_o^3(1+\varepsilon)^3 \Rightarrow V = V_o(1+\varepsilon)^3 \quad (4)$$

The internal diameter of the bladder was assumed to be 68 mm (R = 34 mm), which was the averaged maximum width measured along the circumferential direction of the bladders used in the testing (Figure 1). Moreover, the bladder thickness was assumed to be the averaged group thickness of the bladder strips tested under uniaxial tension.

Results

Histological characterisation

The results of the structural analysis of the bladder wall, obtained from the histological staining of samples from the dorsal, ventral, lateral lower body, and trigone regions, as well as along the apex-to-base and transverse directions, are illustrated in Figure 3 for the non-distended bladders, and Figure 4 and Figure 5 for the bladder fixed while distended to 500 ml. Examination of the regional bladder histioarchitecture revealed that elastin was generally sparse in the bladder wall.

Nevertheless, among the five regions investigated, the samples retrieved from the dorsal, ventral and lateral regions contained the most elastin, whereas the samples from the lower body region contained the least amount of elastin (Figure 3). In all regions, elastin appeared to be oriented predominantly in the transverse (circumferential) direction (Figure 5). In the ventral region, elastin seemed to be concentrated in the lower half/serosa region, whereas the trigone region appeared to contain a scattering of elastin bundles. The detrusor muscle was most compact within the trigone region (Figure 3), but it was difficult to distinguish any discernible patterns of orientation that would discriminate one region from another. Samples retrieved from the lower body and trigone regions of the distended bladder were structurally the least affected by distension, retaining thickness and a convoluted urothelium (Figure 4). Upon distension, the dorsal, lateral and ventral regions reduced in thickness and the local urothelium was flattened. Miller's elastin staining showed the presence of elastin in vessel walls (Figure 5). Van Gieson's staining showed that the muscle bundles in the dorsal, lateral and ventral regions of the distended bladder were more compacted than in the trigone and lower body regions, reflecting the increased distension of these regions and the subsequent reorganisation of the ECM. This supports the observations in the non-distended bladder that the dorsal, ventral and lateral regions contained the most elastin and the lower body region the least. Elastin provides the recoiling mechanism in the tissues and it is usually present in regions of tissues which are subjected to increased deformations. Van Gieson's staining also revealed that the lateral, lower body and trigone regions expressed an increased network of collagen compared to the dorsal and ventral regions (Figure 5).

Biomechanical characterisation

During uniaxial tensile loading to failure, the site of specimen failure was within the central region of the specimens, whereas there was no evidence of specimen slippage within the grips of the holder. The acquired force and elongation data for each specimen tested was converted to stress and strain, respectively, and the averaged apex-to-base and transverse stress-strain behaviours for each of the five regional groups were plotted on the same chart in order to examine the potential directional anisotropy of the bladder wall. These results are illustrated in Figure 6. The average biomechanical parameters obtained from the stress-strain behaviours of the specimens in each of the test groups are gathered in Figure 7. All groups demonstrated the typical quasistatic stress-strain behaviour of soft tissues comprising an initial linear region (elastin phase) followed by a secondary prolonged linear region (collagen phase) before failure. Comparatively to other soft tissues [37], the elastin phase of all groups was much shorter than the extent of the collagen phase, depicting the reduced amount of elastin in the bladder wall, relatively to its content in other ECM structures, observed under histological examination.

Overall, the specimens retrieved along the transverse direction from all regions, appeared to be more compliant, suggesting increased levels of deformation for the same levels of applied stress (Figure 6). However, significant directional anisotropy was present only in the stress-strain behaviour of the lateral, lower body, and trigone regions. Specifically, the lateral region showed significantly increased collagen phase slope ($p = 0.027$) and ultimate tensile strength ($p = 0.013$) along the apex-to-base direction (Figure 7). Statistically significant increase along the apex-to-base direction were also observed in the collagen phase slope ($p = 0.003$), transition stress ($p = 0.027$) and ultimate tensile strength ($p = 0.036$) of the lower body region. The trigone

region presented a significant increase in the collagen phase slope ($p = 0.004$) and significant decrease in the transition ($p = 0.026$) and failure ($p = 0.021$) strains in the apex-to-base direction. In contrast, the dorsal region demonstrated the least directional anisotropy, being in fact, quite isotropic in the whole range of its stress-strain behaviour ($p > 0.05$). In between the two extremes, the ventral region also demonstrated a degree of directional anisotropy, which was limited to a decrease in the transition strain ($p = 0.013$) of the apex-to-base direction.

In order to produce a quantitative comparison of the degree of directional anisotropy between the five anatomical regions, the ratio of the collagen phase slopes between the apex-to-base and transverse direction groups of each of the five regions was calculated and presented in Table 1. These ratios indicated that the lower body region expressed the highest degree of anisotropic behaviour, with a collagen phase slope along the apex-to-base direction more than 3 times bigger than the one along the transverse direction. The smallest ratios were calculated for the dorsal and ventral regions, which demonstrated similar collagen phase slopes along their apex-to-base and transverse directions.

Analysis of the biomechanical parameters also revealed significant regional anisotropy in the bladder wall. However, this anisotropy was confined only in the apex-to-base direction between the five anatomical regions (Figure 7). Statistically significant differences were found in all biomechanical parameters studied except for the case of the elastin phase slope. In the extra-physiological stress range (collagen phase) significant differences were observed in the collagen phase slopes of the dorsal and ventral regions which were reduced compared to the trigone region ($p = 0.020$), and the lateral ($p = 0.043$), lower body ($p = 0.006$) and trigone regions ($p = 0.001$), respectively. This indicated a significantly increased compliance of the dorsal

and ventral compared to the other bladder regions. Moreover, the ultimate tensile strength of the ventral region was significantly reduced compared to the lateral ($p = 0.028$) and lower body ($p = 0.046$) regions, whereas the transition stress of the lower body was significantly increased compared to the dorsal region ($p = 0.483$). With regards to the extensibility of the bladder wall, the trigone region was the least distensible, demonstrating significantly reduced transition and failure strains compared to the dorsal ($p = 0.005$ & 0.004), ventral ($p = 0.017$ & 0.012), lateral ($p = 0.001$ & 0.002), and lower body ($p = 0.001$ & 0.004) regions. The combined findings of this study with regards to the regional anisotropy of the bladder wall along the apex-to-base direction are illustrated in Figure 8, which illustrates the variation of the collagen phase slope, ultimate tensile strength, transition strain and failure strain over the five anatomical regions investigated.

The mesoscale-tissue mechanical properties obtained from the uniaxial tensile tests were correlated to whole bladder mechanics by converting the stress-strain behaviour of each specimen in each of the ten test groups to a pressure-volume response. The purpose was to predict pressure-volume relationships for the whole organ, assuming a regionally and directionally isotropic, homogeneous and spherical bladder. Subsequently, the converted pressure-volume results for each specimen were averaged over the number of specimens in each group and plotted for the physiological bladder volume interval, which was assumed to be ≈ 500 ml (Figure 9). In essence, these pressure-volume relationships represent the behaviour of the whole bladder assuming that its mechanical properties are uniform and identical to the properties of each of the individual test groups. Analysis of these results indicated that there were significant differences in the slopes of the pressure-volume profiles calculated individually for each specimen and averaged for the specimens in each

group (Figure 10). The slope of the model employing the properties of the trigone region along the apex-to-base direction was significantly increased compared to the dorsal (apex-to-base, $p = 0.046$), ventral (transverse, $p = 0.047$), lower body (apex-to-base, transverse; $p = 0.034$ & 0.016, respectively), and trigone (transverse, $p = 0.047$) models.

Discussion

The aim of this study was to investigate the homogeneity and anisotropy of the passive urinary bladder with regards to the mechanical properties and histioarchitecture of the bladder wall. This was the first study, to the knowledge of the authors, which used uniaxial mechanical testing to investigate the regional and directional anisotropy of the urinary bladder, and to correlate the mesoscale-tissue mechanical properties to the whole organ pressure-volume behaviour. Over the years, the quasistatic mechanical properties of the bladder have been characterised utilising tensile loading tests [34,35,42,43,44] and *in vivo* studies [44,45,46,47]. *In vivo* whole organ testing cannot directly determine bladder wall tissue properties due to regional differences, and can be affected by neural influences and intrinsic muscle activity, as well as other concomitant variables such as non-uniform wall stress distribution and external loading by the pelvic organs [35]. Tensile loading tests on bladder wall samples have focused on uniaxial [32,42,43] or biaxial [34,35] protocols. Admittedly, biaxial mechanical testing produces a more physiological loading state as the bladder wall is loaded in all three dimensions *in vivo*. In addition, phenomena such as mechanical cross-coupling, describing how the stress level in one direction can affect the stress-strain behaviour in the other, which can be important in studying biaxial tissues, can be better appreciated under biaxial testing. An improvement to the existing testing methodology would be to employ biaxial testing alongside the

uniaxial protocol. Nevertheless, uniaxial testing is an attractive investigation tool because it localises the investigation to a very small area of the organ from which a tissue sample can be isolated and subjected to controlled stress states. This is a particularly well suited approach when investigating anisotropic behaviour of tissues. Since the purpose of this study was not to fully characterise the mechanical properties of the bladder in terms of a constitutive three-dimensional model, in which case a biaxial testing protocol would be more appropriate, but to investigate its potential anisotropy and inhomogeneity, it was deemed appropriate to use uniaxial tensile testing.

The regional and directional anisotropy of the bladder has attracted surprisingly little attention over the years. A meagre few studies have focused on the anisotropy of the mechanical properties of the bladder [34,35], and even these have concentrated on the directional anisotropy. In addition to the directional anisotropy, this study also identified a regional anisotropy inherent in the mechanical properties of the bladder wall. Moreover, the magnitudes of the biomechanical parameters calculated in this study were comparable to those reported by others for porcine bladder tissue [42], considering the differences in experimental protocols, as well as in the methods used to estimate tissue thickness which have a direct impact on the magnitude of the estimated stress. With regards to the directional anisotropy, the specimens retrieved along the transverse direction from all regions appeared to be more compliant (increased transition and failure strains, reduced collagen phase slopes) compared to the apex-to-base specimens. The increased compliance along the transverse direction, which was more profound in the extra-physiological mechanical properties, indicated that at the organ level the bladder distends more in this direction than along the apex-to-base one. Within the physiological distension

limits (up to approximately the transition point of the stress-strain curve), the increased compliance observed along the transverse direction was supported by the histological results, which indicated that elastin was predominantly oriented in the transverse direction (Figure 5). Elaborating, elastin provides the recoiling mechanism in the tissues and it is most abundant in tissues, or regions of tissues, subject to increased stretching during physiological function [48]. Directional anisotropy was also observed in the ultimate tensile strength of the specimens, with the specimens retrieved along the transverse direction from all regions achieving lower strengths than the apex-to-base specimens. The difference, though, was significant only in the lateral and lower body regions. Overall, the lower body demonstrated the highest degree of directional anisotropy, whereas the dorsal and ventral region demonstrated the least directional anisotropy (Figure 6 & Table1).

Significant regional anisotropy in the bladder wall was found only along the apex-to-base direction (Figure 7 & 8). The lack of any significant regional anisotropy along the transverse direction indicates that the organ experiences a rather uniform circumferential expansion. Statistically significant differences were found in all biomechanical parameters except in the slope of the elastin phase. The dorsal and ventral regions demonstrated a significantly increased compliance along the longitudinal direction compared to the other bladder regions, as indicated by the reduced collagen phase slope and transition stress, and increased transition and failure strain of these regions. The reduced transition stress of these regions indicates that they can reach their transition point, at which the collagen and smooth muscle fibres have uncrimped and begin to bear all the applied load, with less effort (less pressure) than the other regions. As a complementary effect, the significantly increased transition strain of the dorsal and ventral regions, as well as of the lateral

region, compared to the trigone, indicates that with the same effort (same pressure) these regions are prone to deform more than the trigone in the apex-to-base direction. In fact, the trigone region demonstrated the least distensibility, experiencing the lowest transition and failure strains and the highest collagen phase slope in both directions (although not significantly so in the transverse) compared to the other regions (Figure 7 & 8). The second highest collagen phase slope and lowest failure strain was demonstrated by the lower body region. The findings of the increased compliance of the dorsal, ventral and lateral regions compared to the trigone and lower body regions were supported by the increased elastin network found in these regions, as well as by the fact that histological samples retrieved from the lower body and trigone regions of the distended bladder were structurally the least affected by distension. The trigone, lower body and lateral regions also demonstrated the highest tensile strength both at regional and directional level. This can be attributed to the increased networks of collagen, the main function of which in connective tissues is to withstand tension, as well as to the thicker layers of muscle, observed in these regions under histological examination.

The directional and regional anisotropy in the mesoscale-tissue mechanical properties of the bladder was inherited in the whole organ mechanics when the stress-strain behaviours of the different regions were used to model pressure-volume relationships for the whole organ. The purpose was to investigate whether mesoscale-tissue mechanical properties can be translated to meaningful whole organ mechanics, given an appropriate model for the bladder shape and how the wall stretch is distributed in the bladder wall. The assumptions of a spherical geometry, homogeneity and anisotropy do not constitute a realistic bladder model. Nevertheless, this model was sufficient to examine how the whole pressure-volume

relationship of bladder changes if the mechanical properties of a particular bladder region are adopted as universal bladder properties. Although these results were at best estimates based on assumptions of homogeneity, and only descriptive of whole bladder mechanics, they were indicative of the inherent regional and directional anisotropy present in the bladder. The modelled pressure-volume profiles were in general agreement with similar data obtained from bladder cystometry [49]. However, there was a considerable scatter among the results of the individual regions and directions. The scatter ranged from a model describing a bladder that offers considerable resistance to deformation, by employing the results of the trigone region along the apex-to-base direction, to a bladder that is quite compliant and offers little resistance to deformation, by employing the results of the ventral region along the transverse direction. Moreover, the pressure-volume models verified the lack of any significant anisotropy along the transverse direction of the anatomical regions, with the models assuming the properties of the transverse regional groups clustering together, towards the compliant bladder region.

Conclusions

This study detected significant regional and directional anisotropy in the quasistatic uniaxial mechanical properties of the passive urinary bladder and correlated this anisotropy to the distended and non-distended tissue histioarchitecture and whole organ mechanics. The experimental protocol used to evaluate the mesoscale mechanical properties of the bladder by employing uniaxial tensile testing was effective in detecting bladder anisotropy. Differences between isotropic and anisotropic behaviour can become important in regions of high stress and in bladder augmentation surgery that changes the natural shape and boundary conditions of the bladder. In general, the results from this study will aid the regional

differentiation of bladder treatments in terms of partial bladder replacement, as well as the development of more realistic constitutive models of bladder wall biomechanics and improved computational simulations to predict deformations in the natural and augmented bladder.

Acknowledgements

This work was funded by the Biotechnology and Biological Sciences Research Council (BBSRC Grant E20352). SK is funded by the Engineering and Physical Sciences Research Council.

References

1. Chang SL, Chung JS, Yeung MK, Howard PS, Macarak EJ. Roles of the lamina propria and the detrusor in tension transfer during bladder filling. Scand J Urol Nephrol Suppl 1999; 201:38-45.

2. Elbadawi A, Meyer S, Regnier CH. Role of ischemia in structural changes in the rabbit detrusor following partial bladder outlet obstruction: a working hypothesis and a biochemical/structural model proposal. Neurourol Urodynam 1989; 8: 151-162.

3. Gabella G. Hypertrophy of visceral smooth muscle. Anat Embryol 1990; 182:409-424.

4. Kitada S, Wein AJ, Kato K, Levin RM. Effect of acute complete obstruction on the rabbit urinary bladder. J Urol 1989; 141: 166-169.

5. Tammela TLJ, Levin RM, Monson FC, Wein AJ, Longhurst PA. The influence of acute over-distension on rat bladder function and DNA synthesis. J Urol 1993; 150:15331539.

6. German K, Bedwani J, Davies J, Brading AF, Stephenson TP. An assessment of the contribution of visco-elastic factors in the aetiology of poor compliance in the human neuropathic bladder. Br J Urol 1994; 74(6):744-748.

7. Watanabe T, Rivas DA, Chancellor MB. Urodynamics of spinal cord injury. Urol Clin North Am 1996; 23(3):459-473.

8. Kruse MN, Bray LA, de Groat WC. Influence of spinal cord injury on the morphology of bladder afferent and efferent neurons. J Auton Nerv Syst 1995; 54(3):215-224.

9. Bunyaratavey P, Lao S, Kongkanand A, Brasopsanti K, Vajarapongse R. Ten years' experience with enterocystoplasty. J Med Assoc Thai 1993; 76: 327–333.

10. Khoury JM, Timmons SL, Corbel L, Webster GD. Complications of enterocystoplasty. Urology 1992; 40: 9–14.

11. Greenwell TJ, Venn SN, Mundy AR. Augmentation cystoplasty. BJU Int. 2001; 88(6):511-25.

12. Chancellor MB, Rivas DA, Bourgeois IM. Laplace's law and the risks and prevention of bladder rupture after enterocystoplasty and bladder autoaugmentation. Neurourol Urodyn 1996;15(3):223-233.

13. Bolland F, Korossis S, Wilshaw SP, Ingham E, Fisher J, Kearney JN *et al*. Development and characterisation of a full-thickness acellular porcine bladder matrix for tissue engineering. Biomaterials 2007 Feb; 28(6):1061-1070.

14. Southgate J, Cross W, Eardley I, Thomas DF, Trejdosiewicz LK. Bladder reconstruction-from cells to materials. Proc Inst Mech Eng [H]. 2003; 217(4):311-316.

15. Korossis S, Bolland F, Ingham E, Fisher J, Kearney J, Southgate J. Review: tissue engineering of the urinary bladder: considering structure-function relationships and the role of mechanotransduction. Tissue Eng 2006; 12(4):635-644.

16. Roelofs M, Wein AJ, Monson FC, Passeriniglazel G, Koteliansky VE, Sartore S *et al*. Contractility and phenotype transitions in serosal thickening of obstructed rabbit bladder. J Appl Physiol 1995; 78: 1432–41.

17. Wang Z, Gopalakurup SK, Levin RM, Chacko S. Expression of smooth muscle myosin isoforms in urinary bladder smooth muscle during hypertrophy and regression. Lab Invest 1995; 73: 244–51.

18. Baskin LS, Constantinescu S, Duckett JW, Snyder HM, Macarak E. Type III collagen decreases in normal foetal bovine bladder development. J Urol 1994; 152: 688–91.

19. Landau EH, Jayanthi VR, Churchill BM, Shapiro E, Gilmour RF, Khoury AE *et al*. Loss of elasticity in dysfunctional bladders: urodynamic and histochemical correlation. J Urol 1994; 152: 702–5.

20. Venegas JG. Viscoelastic properties of the contracting detrusor: I. theoretical basis. Am J Physiol 1991; 261:C355–363.

21. Finkbeiner AE, O'Donnell PD. Responses of detrusor smooth muscle to stretch and relaxation: in vitro study. Urology 1990; 36: 193–198.

22. Regnier CH, Kolsky H, Richardson PD, Ghoniem GM, Susset JG. The elastic behavior of the urinary bladder for large deformations. J Biomech 1983; 16: 915–922.

23. Coolsaet BL, van Mastrigt R, Van Duyl WA, Huygen RE. Viscoelastic properties of bladder wall strips at constant elongation. Invest Urol 1976; 13: 435–440.

24. Coolsaet BL, van Duyl WA, van Mastrigt R, van der Zwart A. Visco-elastic properties of the bladder wall. Urol Int 1975; 30: 16–26.

25. Alexander RS. Viscoplasticity of smooth muscle of urinary bladder. Am J Physiol 1973; 224: 618–622.

26. Kondo A, Susset JG. Physical properties of the urinary detrusor muscle. A mechanical model based upon the analysis of stress relaxation curve. J Biomech 1973; 6: 141–151.

27. Klevmark B. Motility of the urinary bladder in cats during filling at physiological rates. I. Intravesical pressure patterns studied by a new method of cystometry. Acta Physiol Scand 1974; 90: 565–577.

28. Klevmark B. Motility of the urinary bladder in cats during filling at physiological rates. II. Effects of extrinsic bladder denervation on intramural tension and on intravesical pressure patterns. Acta Physiol Scand 1977; 101: 176–184.

29. Tözeren A. Assessment of fibber strength in a urinary bladder by using experimental pressure volume curves: an analytical method. J Biomech Eng 1986; 108:301-305.

30. Van Mastrigt R, Griffiths DJ. An evaluation of contractility parameters determined from isometric contractions and micturition studies. Ural Res 1986; 14:45-52.

31. Damaser MS, Lehman SL. The effect of urinary bladder shape on its mechanics during filling. J Biomechanics 1995; 28(6):725-732.

32. Andersson KE, Arner A. Urinary bladder contraction and relaxation: physiology and pathophysiology. Physiol Re 2004; 84:935-986.

33. Gabella G, Uvelius B. Urinary bladder of rat: fine structure of normal and hypertrophic musculature. Cell Tissue Res 1990; 262:67–79.

34. Gloeckner D, Sacks M, Chancellor M, de Groat W. Active and passive biaxial mechanical properties of urinary bladder wall. In: Engineering in Medicine and Biology. 21st Annual Conf. and the 1999 Annual Fall Meeting of the Biomedical Engineering Society BMES/EMBS Conference. 1999; 1:17.

35. Gloeckner DC, Sacks MS, Fraser MO, Somogyi GT, de Groat WC, Chancellor MB. Passive biaxial mechanical properties of the rat bladder wall after spinal cord injury. J Urol. 2002; 167(5):2247-2252.

36. Southgate J, Masters JR, Trejdosiewicz LK. Culture of human urothelium. In: Freshney RI FM, editor. Culture of epithelial cells. 2nd ed. New York: Wiley. 2002; 381–400.

37. Korossis S, Booth C, Wilcox HE, Watterson KG, Kearney JN, Ingham E *et al*. Tissue engineering of cardiac valve prostheses II: Biomechanical characterisation of decellularised porcine aortic heart valves. J Heart Valve Dis. 2002; 11(4):463-471.

38. Bancroft J, Stevens A. Theory and practice of histological techniques. London: Churchill Livingstone. 1990.

39. Korossis S, Wilcox HE, Watterson KG, Kearney JN, Ingham E, Fisher J. In-vitro assessment of the functional performance of the decellularised intact porcine aortic root. J Heart Valve Dis. 2005; 14(3):408-422.

40. Griffiths CJ, Assi MS, Styles RA, Ramsden PD, Neal DE. Ambulatory monitoring of bladder and detrusor pressure during natural filling. J Urol 1989; 142:780–784.

41. Fung YCB. Biomechanics, mechanical properties of living tissues. 2nd ed, Springer-Verlag, New York 1993; 14-20.

42. Dahms E, Piechota HJ, Dahiya R Lue TF, Tanagho EA. Composition and biomechanical properties of the bladder acellular matrix graft: comparative analysis in rat, pig and human. Br J Urol 1998; 82:411-419.

43. Alexander RS. Series elasticity of urinary bladder smooth muscle. Am J Physiol 1976; 231:1337.

44. Alexander RS. Mechanical properties of urinary bladder. Am J Physiol 1971; 220:1413.

45. Rohrmann D, Zderic SA, Duckett JW, Levin RM, Damaser MS. Compliance of the obstructed foetal rabbit bladder. Neurourol Urodyn 1997; 16(3):179-189.

46. Coplen DE, Macarak EJ, Levin RM. Developmental changes in normal foetal bovine whole bladder physiology. J Urol 1994; 151:1391.

47. Levin RM, Horan P, Liu SP. Metabolic aspects of urinary bladder filling. Scand J Urol Nephrol suppl. 1999; 201:59.

48. Viidik A, Danielsen CC, Oxlund H. On fundamental and phenomenological models, structure and mechanical properties of collagen and elastin and glycosaminoglycan complexes. Biorheology 1982; 19: 437–451.

49. Damaser MS. Whole bladder mechanics during filling. Scand J Urol Nephrol Suppl 1999; 201:51–58

Figure1

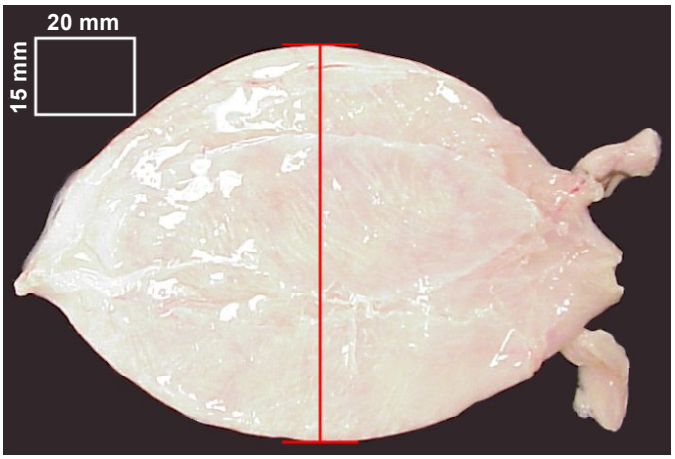

Figure 2

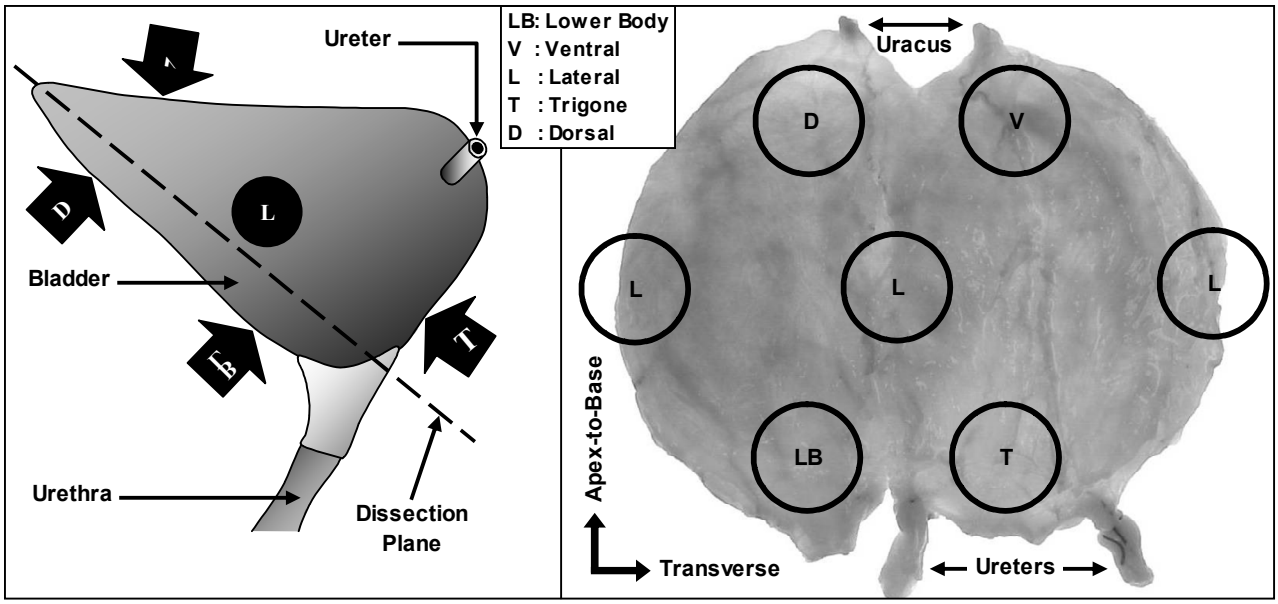
LB: Lower Body
V : Ventral
L : Lateral
T : Trigone
D : Dorsal
Ureter
V
D
L
Bladder
LB
T
Urethra
Dissection Plane
(a)
Uracus
D
V
L
L
L
LB
T
Apex-to-Base
Transverse
Ureters
(b)

Figure 3

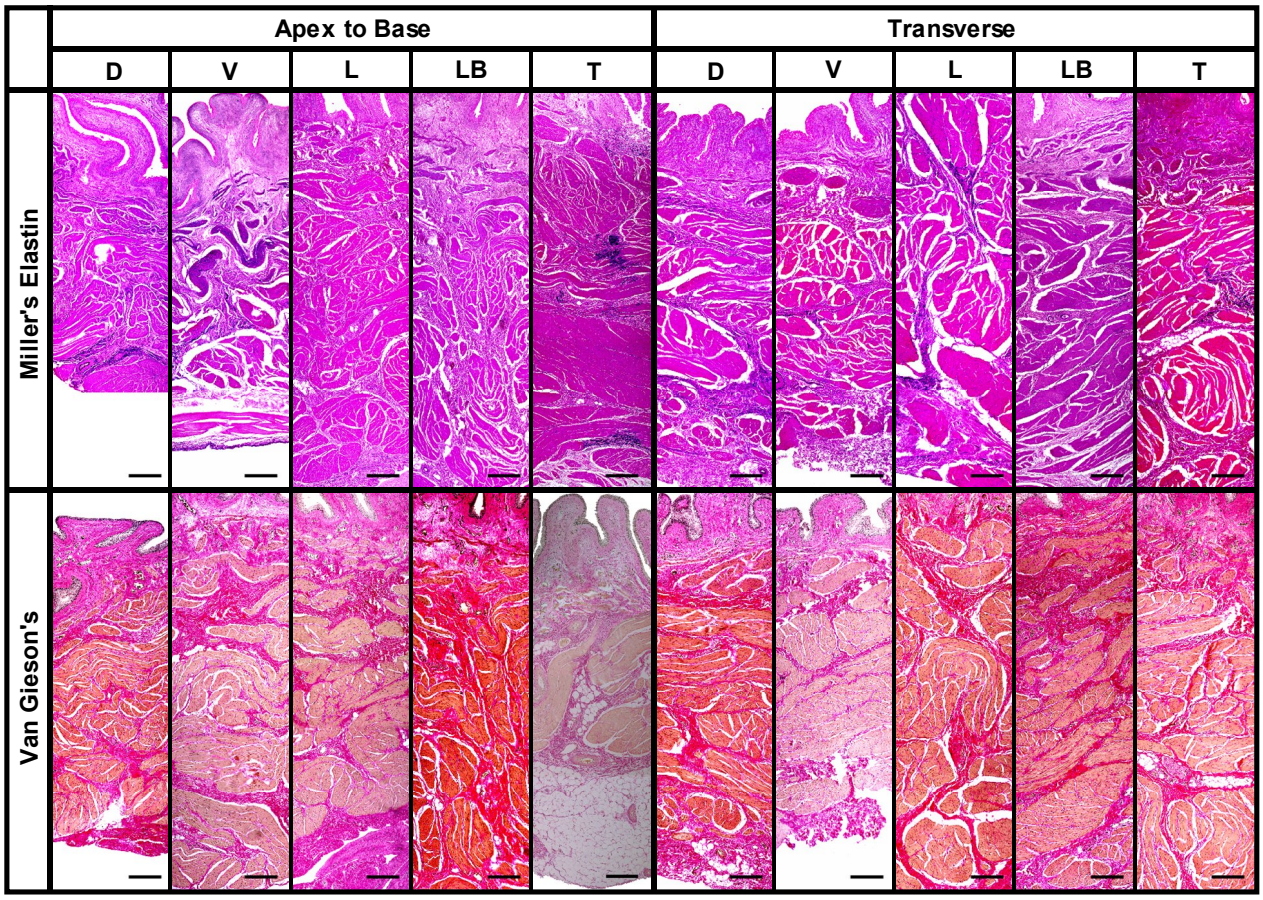
Apex to Base
Transverse
D
V
L
LB
T
D
V
L
LB
T
Miller's Elastin
Van Gieson's

Figure 4

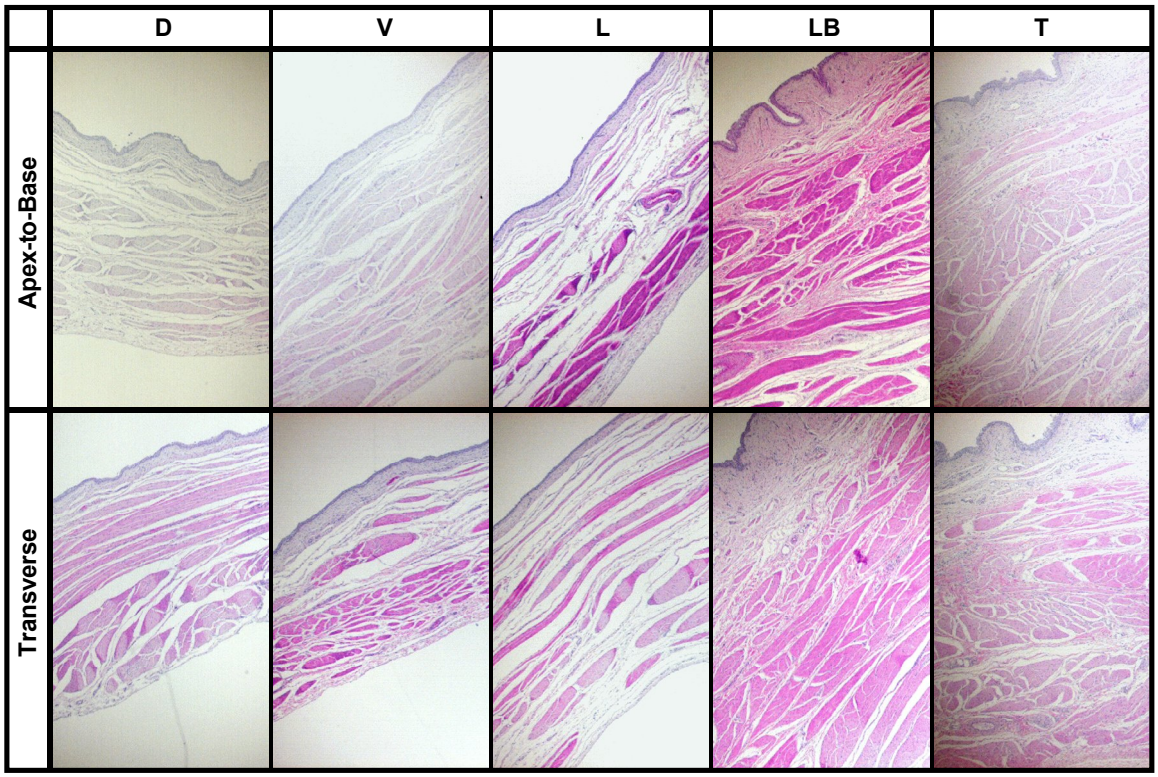

Figure 5

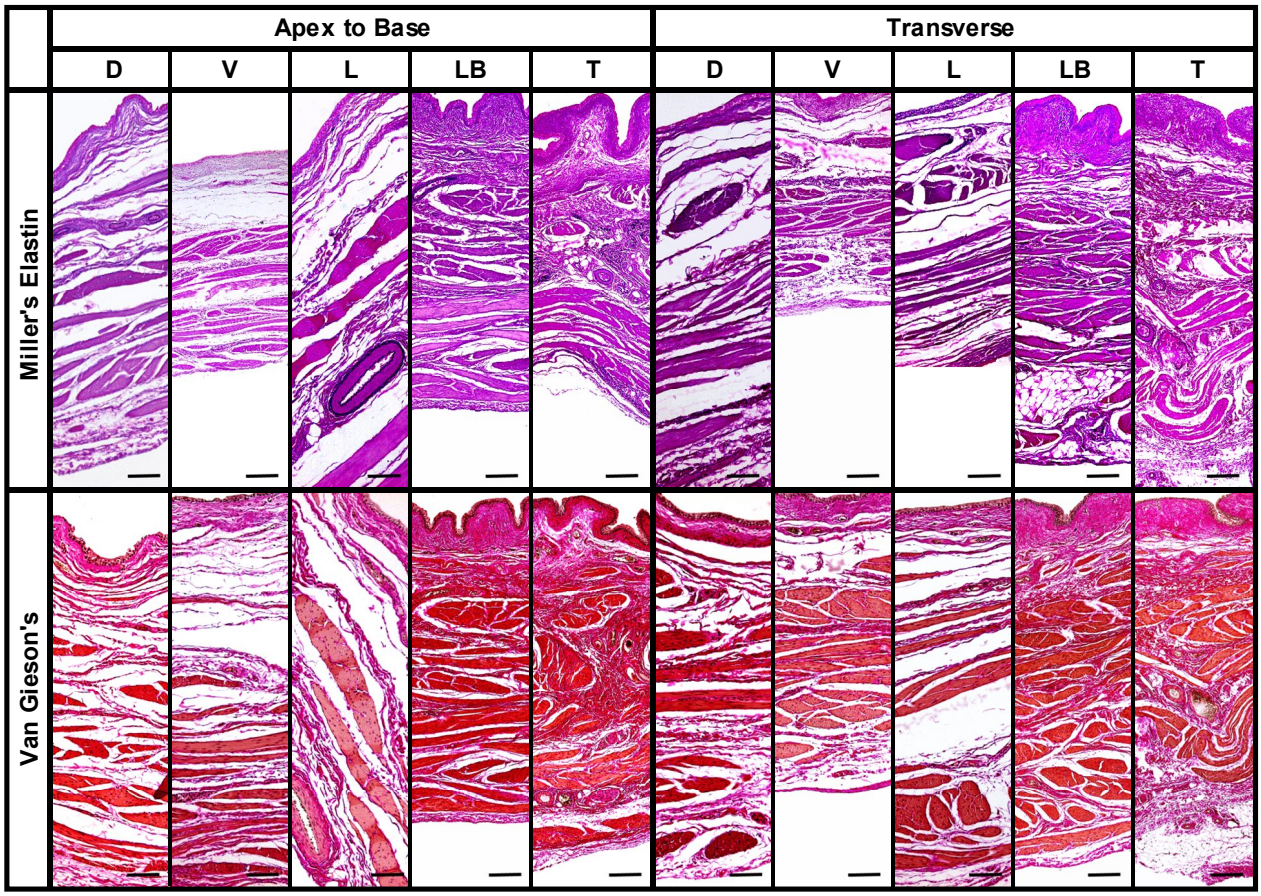
Apex to Base
Transverse
D
V
L
LB
T
D
V
L
LB
T
Miller's Elastin
Van Gieson's

Figure 6

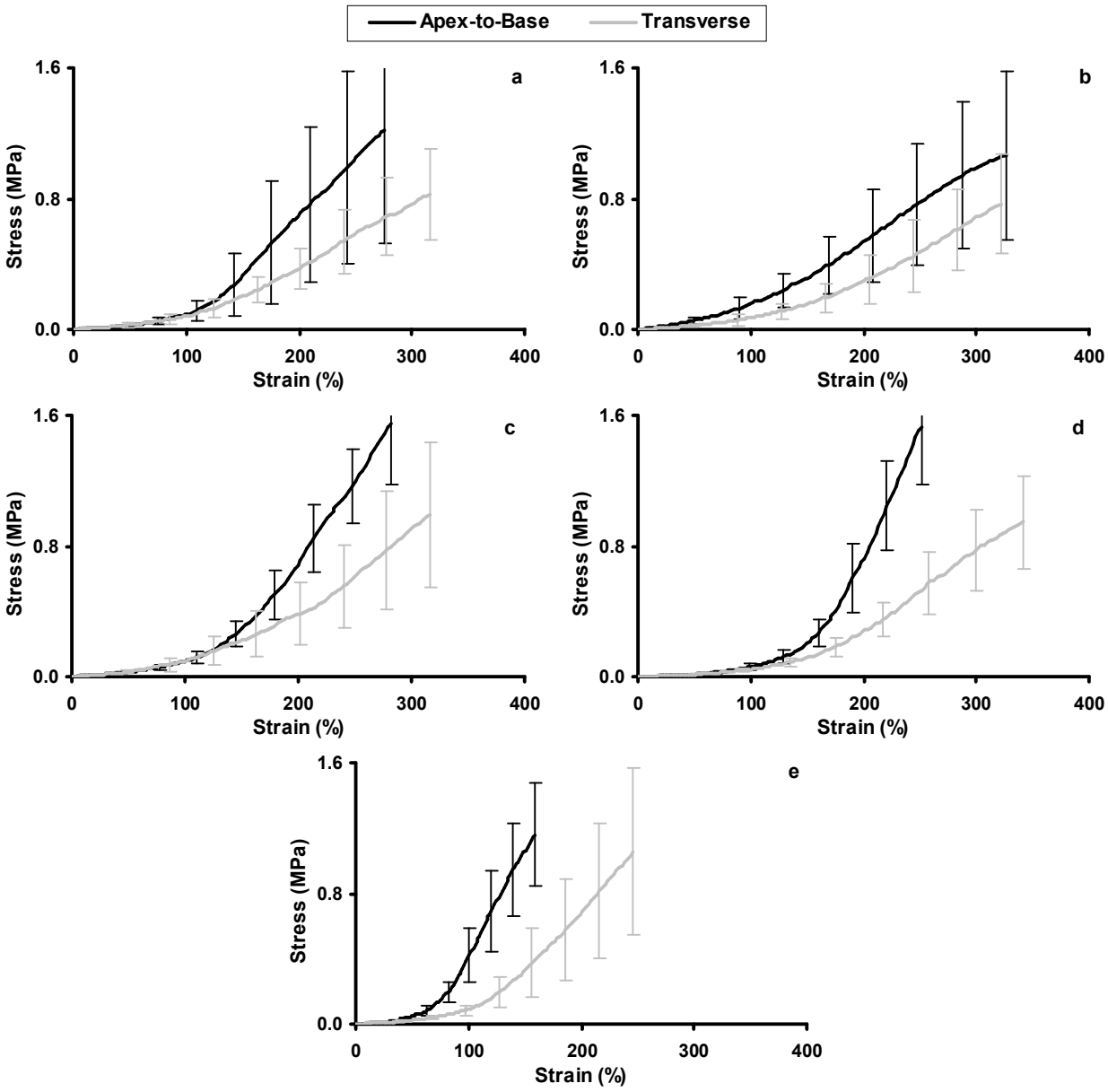
Apex-to-Base
Transverse
a
b
c
d
e
Stress (MPa)
Strain (%)
0.0
0.8
1.6
0
100
200
300
400

Figure 7

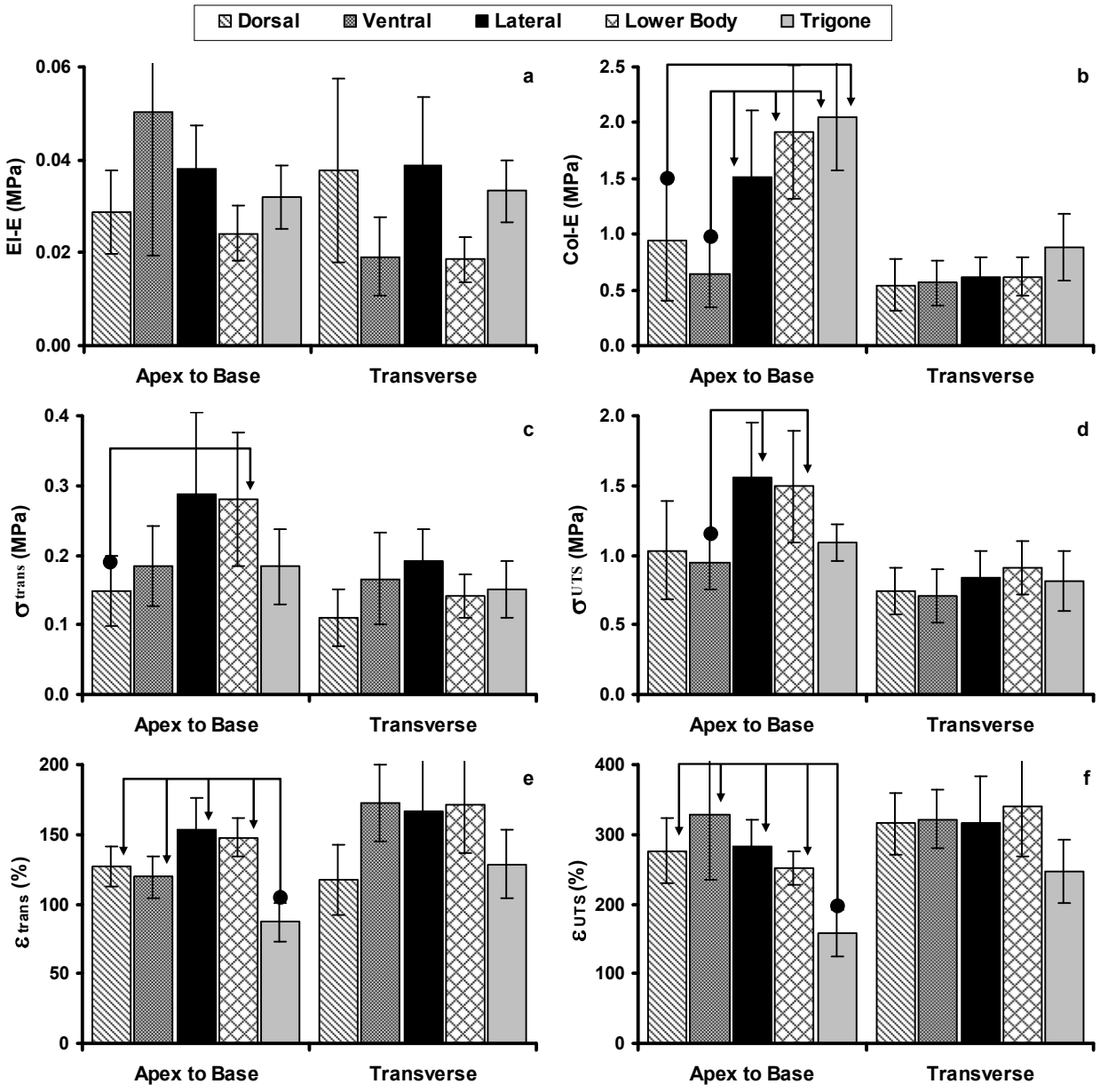
Dorsal
Ventral
Lateral
Lower Body
Trigone
a
El-E (MPa)
0.06
0.04
0.02
0.00
Apex to Base
Transverse
b
Col-E (MPa)
2.5
2.0
1.5
1.0
0.5
0.0
Apex to Base
Transverse
c
σ trans (MPa)
0.4
0.3
0.2
0.1
0.0
Apex to Base
Transverse
d
σ UTS (MPa)
2.0
1.5
1.0
0.5
0.0
Apex to Base
Transverse
e
ε trans (%)
200
150
100
50
0
Apex to Base
Transverse
f
ε UTS (%)
400
300
200
100
0
Apex to Base
Transverse

Figure 8

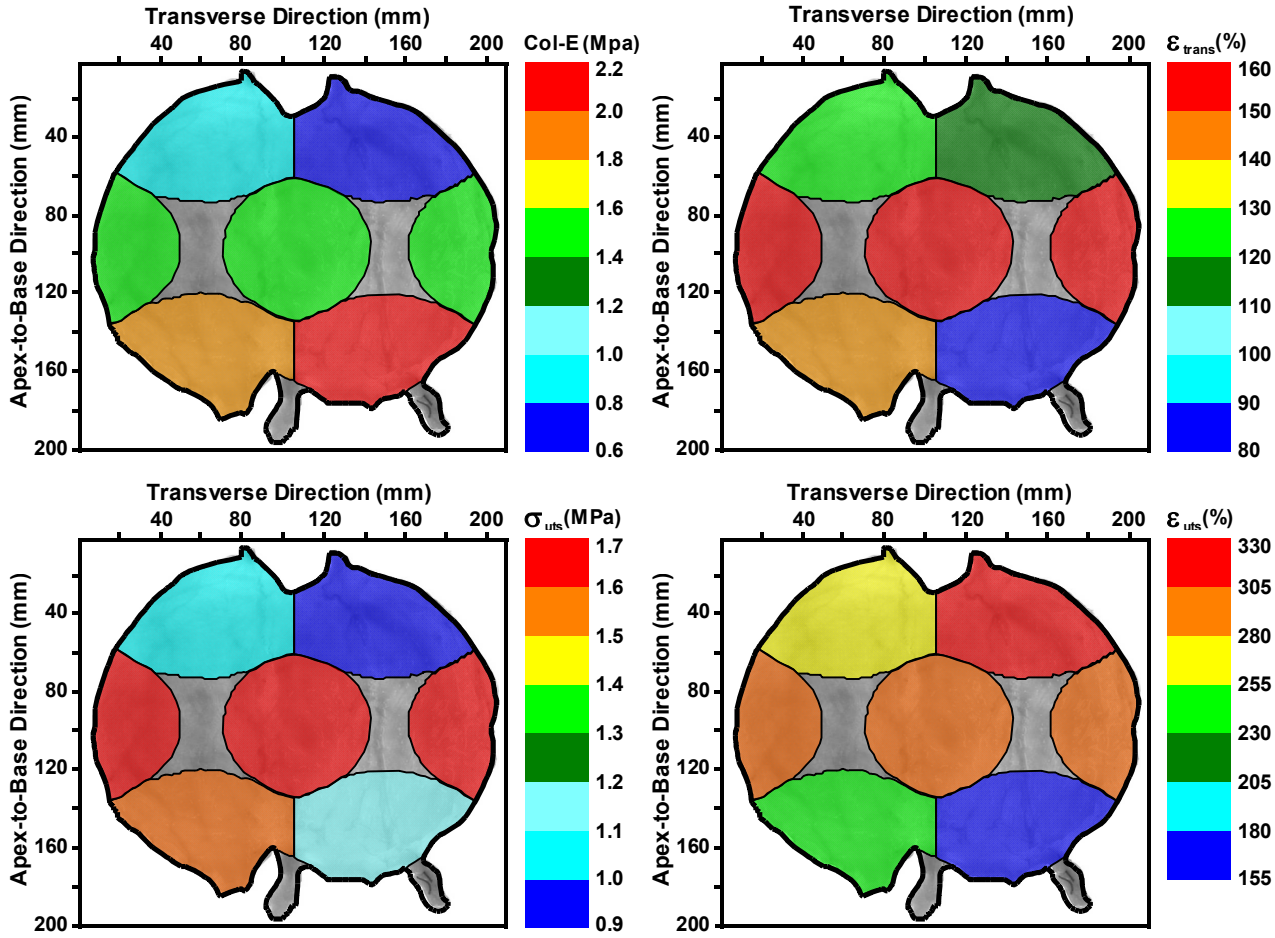
Transverse Direction (mm)
40
80
120
160
200
Apex-to-Base Direction (mm)
CoI-E (Mpa)
2.2
2.0
1.8
1.6
1.4
1.2
1.0
0.8
0.6
ε trans(%)
160
150
140
130
120
110
100
90
80
σ uts(MPa)
1.7
1.6
1.5
1.4
1.3
1.2
1.1
1.0
0.9
ε uts(%)
330
305
280
255
230
205
180
155

Figure 9

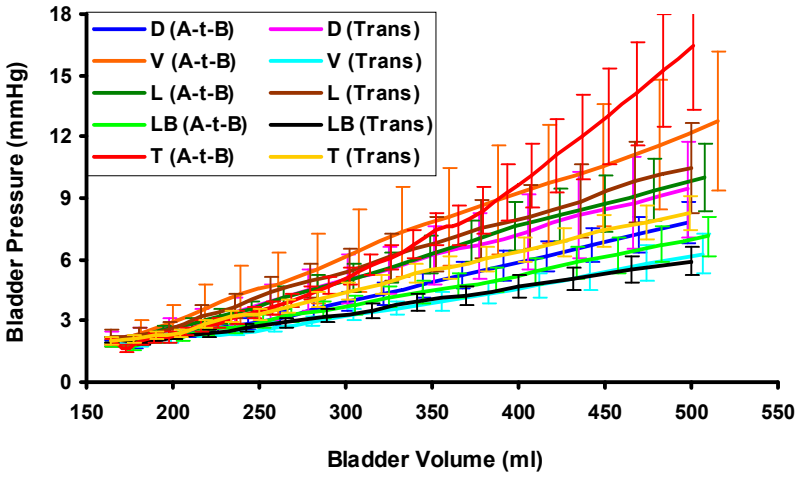
D (A-t-B)
V (A-t-B)
L (A-t-B)
LB (A-t-B)
T (A-t-B)
D (Trans)
V (Trans)
L (Trans)
LB (Trans)
T (Trans)
Bladder Pressure (mmHg)
0
3
6
9
12
15
18
150
200
250
300
350
400
450
500
550
Bladder Volume (ml)

Figure 10

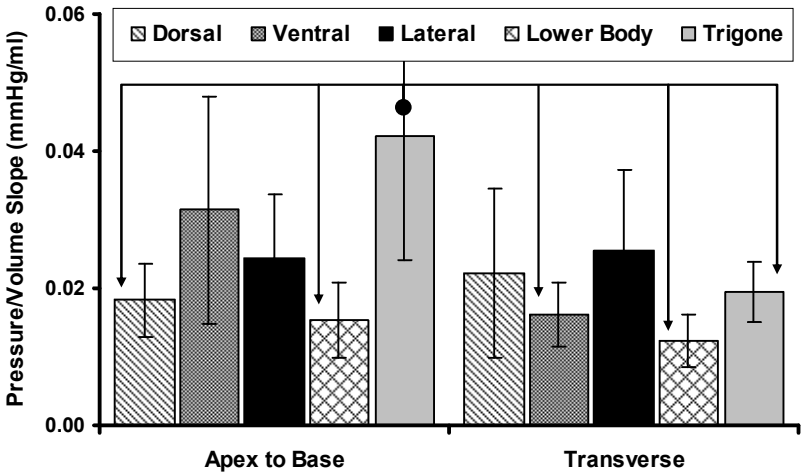
Dorsal
Ventral
Lateral
Lower Body
Trigone
Pressure/Volume Slope (mmHg/ml)
0.06
0.04
0.02
0.00
Apex to Base
Transverse

Figure Captions

Figure 1: Bladder sizing. Bladder width was measured along the transverse line.

Figure 2: Bladder dissection and sample localization. (a) Schematic of bladder in the anterior-posterior plane; (b) Cut-opened porcine bladder showing the anatomical map of the five anatomical regions investigated

Figure 3: Staining of full thickness samples retrieved from the dorsal (D), ventral (V), lateral (L), lower body (LB) and trigone (T) regions of non-distended bladder (luminal side up). Bar: 250 μm.

Figure 4: H & E staining of full thickness samples retrieved from the dorsal (D), ventral (V), lateral (L), lower body (LB) and trigone (T) regions of distended bladder (4× magnification).

Figure 5: Staining of full thickness samples retrieved from the dorsal (D), ventral (V), lateral (L), lower body (LB) and trigone (T) regions of distended bladder. Bar: 250 μm.

Figure 6: Regional mean stress-strain behaviour of the bladder wall along the apex-to-base and transverse directions (error bars indicate the 95% confidence intervals, n = 6): a) dorsal; b) ventral; c) lateral; d) lower body; e) trigone.

Figure 7: Regional mean biomechanical parameters of the bladder wall along the apex-to-base and transverse directions (error bars indicate the 95% confidence intervals, n = 6): a) elastin phase slope (El-E); b) collagen phase slope (Col-E); c) transition stress (σ_{trans}); d) ultimate tensile strength (σ_{uts}); e) transition strain (ε_{trans}); f) failure strain (ε_{uts}). Connectors indicate significant ($p<0.05$) regional difference between originator column and end arrow column.

Figure 8: Regional topographic map of the urinary bladder showing the variation of the mean collagen phase slope (Col-E), ultimate tensile strength (σ_{uts}), transition strain (ε_{trans}), and failure strain (ε_{uts}) over the five anatomical regions investigated, and along the apex-to-base direction. These results correspond to the results presented in Figure 6.

Figure 9: Mean pressure-volume profiles calculated from the stress-strain behaviour of the dorsal (D), ventral (V), lateral (L), lower body (LB), and trigone (T) bladder regions along the apex-to-base and transverse directions (mean ± 95% confidence interval, n = 6).

Figure 10: Average slopes of the pressure-volume profiles for the dorsal, ventral, lateral, lower body, and trigone models (error bars indicate the 95% confidence intervals, n = 6). Connectors indicate significant difference.

Table 1

Ratios of Col-E between the apex-to-base and transverse direction groups.

Bladder Region:	Dorsal	Ventral	Lateral	Lower Body	Trigone
Col-E Ratio :	1.4	1.2	2.5	3.1	2.5